Biology of Reproduction, 2017, 96(6), 1167–1180
doi:10.1093/biolre/iox044
Research Article
Advance Access Publication Date: 8 May 2017

OXFORD

Research Article

MicroRNA-21 plays a pivotal role in the oocyte-secreted factor-induced suppression of cumulus cell apoptosis†

Xiao Han, Rui Xue, Hong-Jie Yuan, Tian-Yang Wang, Juan Lin, Jie Zhang, Bo Liang and Jing-He Tan

College of Animal Science and Veterinary Medicine, Shandong Agricultural University, Tai-an City, Shandong Province, P. R. China

*__Correspondence:__ College of Animal Science and Veterinary Medicine, Shandong Agricultural University, Tai-an City 271018, Shandong Province, P. R. China. Tel: +0538-8249616; Fax: +0538-8241419; E-mail: tanjh@sdau.edu.cn

†__Grant Support:__ This study was supported by grants from the National Basic Research Program of China (nos. 2014CB138503 and 2012CB944403) and the China National Natural Science Foundation (nos. 31272444 and 30972096).

Received 24 April 2017; Accepted 8 May 2017

Abstract

It is known that oocytes and cumulus cells (CCs) are more resistant to apoptosis than other compartments of the antral follicle. However, although oocyte-secreted factors (OSFs) have been found to be involved in suppressing bovine CC apoptosis, little is known about the intracellular mechanisms by which OSFs render CCs resistant to apoptosis. Here, we show that coculture with mouse or pig cumulus-denuded oocytes, culture with recombinant mouse growth differentiation factor-9 (GDF-9), or culture in pig oocyte-conditioned medium (POCM) significantly inhibited CC apoptosis of mouse oocytectomized cumulus oophorus complexes (OOXs). The POCM contained both GDF-9 and bone morphogenetic protein-15, and their levels remained constant during culture of OOXs. The level of microRNA-21 (miR-21) was significantly lower in OOXs than in COCs after culture in a simplified α-MEM medium, but increased significantly when OOXs were cultured with GDF-9 or in POCM. The level of miR-21 in OSF-treated CCs was correlated with that of Dicer1 but not that of Drosha mRNA. Inhibiting activin receptor-like kinase 5 or SMAD3 completely abolished the beneficial effects of GDF-9 or POCM on CC apoptosis and miR-21 levels. Up- and downregulating miR-21 expression significantly reduced and increased CC apoptosis, respectively. The OSF-upregulated miR-21 expression suppressed CC apoptosis with activation of the PI3K/Akt signaling. In conclusion, miR-21 plays a pivotal role in the OSF suppression of CC apoptosis. OSFs upregulated miR-21 expression through the TGF-β superfamily signaling, which worked through DICER. MicroRNA-21 prevented apoptosis via the PI3K/Akt signaling.

Summary Sentence

MicroRNA-21 plays a pivotal role in the oocyte-secreted factor suppression of cumulus cell apoptosis to explore the intracellular mechanisms by which oocyte-secreted factors suppress cumulus cell apoptosis.

Key words: microRNA, oocyte-secreted factors, GDF-9, cumulus cells, apoptosis.

Introduction

In mammalian ovaries, the antral follicles contain two types of granulosa cells that are anatomically and functionally different, whereas the mural granulosa cells line the wall of the follicle, the cumulus cells (CCs) surround the oocyte, forming the so-called cumulus-oocyte complexes (COCs). Although many antral follicles continue to grow after leaving the primordial follicle pool, only very small numbers ever ovulate, and most of them die by the process of

follicle atresia [1]. During the atresia of antral follicles, the first signs are the presence of pyknotic nuclei indicative of apoptosis in the mural granulosa cells and antrum [1–5]. Then, the theca cells undergo hypertrophy with reduced androsterone production [6]. The CCs and the oocyte are affected only at the most advanced stages of atresia [3,7,8]. To explore why oocytes and CCs are more resistant to apoptosis than other compartments of the antral follicle, Hussein et al. [9] demonstrated that oocyte-secreted bone morphogenetic protein (BMP)-15 and -6 were involved in maintaining a low incidence of bovine CC apoptosis. However, the intracellular mechanisms by which BMPs endow CCs with the apoptosis-resistance are largely unknown. Furthermore, although it is known that mouse oocytes express both BMP-15 and growth differentiation factor (GDF)-9 [10,11], whether these two growth factors play any role in suppressing mouse CC apoptosis has yet to be studied.

GDF-9 and BMP-15 are oocyte-secreted factors (OSFs) of the transforming growth factor β (TGF-β) superfamily that are expressed in growing oocytes throughout all stages of folliculogenesis and in COCs after ovulation [12–14]. GDF-9 and BMP-15 have been shown to signal through TGF-β superfamily receptors to activate the Sma- and Mad-related protein (SMAD) intracellular cascade in granulosa cells [15]. Specifically, whereas BMP-15 binds the BMP type-II receptor (BMPR-II) and activin receptor-like kinase (ALK) 6, activating SMAD1/5/8, GDF-9 binds BMPR-II and ALK5, activating SMAD2/3. The activated SMAD1/5/8 or SMAD2/3 then associate with SMAD4, and the resulting complex translocates to the nucleus to regulate the expression of target genes.

MicroRNA (miRNA) is a group of genome-encoded, single-strand, small molecule (~22 nt), and noncoding RNAs that are involved in a diverse of cellular processes. The expression of miRNAs in CCs has been reported in various mammalian species including human [16], bovine [17], mice [18], and pig [19]. There are many reports on the antiapoptotic effects for some miRNAs. For example, markedly elevated levels of microRNA-21 (miR-21) were observed in human glioblastoma cells [20], glioblastoma multiforme cells [21] and breast tumor tissues [22], and knockdown of miR-21 in cultured cells of these tumor tissues triggered activation of caspases and led to increased apoptosis. Although overexpression of miR-21 promoted proliferation and invasion while inhibiting apoptosis, anti-miR-21 yielded apoptotic effects in colorectal cancer cells [23]. Furthermore, miR-21 blocked apoptosis in mouse periovulatory granulosa cells [24]. However, it is not known whether miRNAs are involved in the inhibition of CC apoptosis mediated by OSFs.

In human vascular smooth muscle cells, TGF-β and BMP signaling promotes a rapid increase in the expression of mature miR-21 via promoting the processing of primary transcripts of miR-21 (pri-miR-21) into precursor miR-21 (pre-miR-21) by the DROSHA complex [25]. The TGF-β- and BMP-specific SMAD signal transducers are recruited but SMAD4 is not required for this process. Furthermore, Zhong et al. [26] observed that the Smad3 signaling, but not Smad2 signaling, increases the expression of miR-21, which promotes renal fibrosis. There are also reports that GDF-9 and miR-21 suppress cell apoptosis through activation of the PI3K/Akt signaling pathway. In porcine CCs, for example, GDF-9 maintained a low level of BIMEL expression and prevented apoptosis by activating the PI3K/FOXO3a pathway [27]. In mice, preantral follicular granulosa cells inhibited oocyte apoptosis through the GDF9-PI3K-Akt signaling pathway [28]. Furthermore, studies in other somatic cells also indicate that miR-21 inhibited apoptosis by upregulating the PI3K/Akt signaling pathway [29–31].

From the above literature review, we proposed that miR-21 would play a pivotal role in the OSF suppression of CC apoptosis. Thus, OSFs would upregulate miR-21 expression through the TGF-β superfamily signaling and the elevated miR-21 would suppress apoptosis of CCs by activating the PI3K/Akt signaling. Experiments were conducted to test this hypothesis. Firstly, roles of OSFs and miR-21 in suppressing CC apoptosis were determined by comparing apoptotic parameters and miR-21 levels in CCs between cultured mouse COCs and oocytectomized cumulus oophorus complexes (OOXs), and by observing the effects of coculture of mouse OOXs with mouse or pig cumulus-denuded oocytes (DOs), culture with GDF-9 supplementation or culture in pig oocyte-conditioned medium (POCM) on CC apoptotic parameters and miR-21 levels. Secondly, whether OSFs inhibit CC apoptosis by activating the TGF-β superfamily signaling was verified by observing the effects of inhibiting ALK5 or SMAD3 on CC apoptosis and miR-21 expression in OOXs cultured in the presence of OSFs. Thirdly, miR-21 expression was up- and downregulated in mouse CCs, and the effect on the apoptotic parameters was examined to further confirm the role of miR-21 in preventing CC apoptosis. Fourthly, whether the TGF-β superfamily signaling promotes miR-21 processing through DROSHA or DICER was determined by observing the effects of OSF treatment on CCs expression of DROSHA and DICER mRNAs. Finally, the mechanism by which miR-21 inhibits CC apoptosis was explored by inhibiting the PI3K/Akt pathway in CCs with miR-21 upregulated with GDF-9 or by miR-21 mimic transfection.

Materials and methods

Unless otherwise specified, all chemicals and reagents used were purchased from Sigma Chemical Co. (St. Louis, MO, USA).

Mice and oocyte recovery

Mice of the Kunming breed were kept in a room with 14L:10D cycles, with the dark period starting from 20:00. The experimental procedures used for animal care and handling were approved by the Animal Care and Use Committee of the Shandong Agricultural University, P. R. China (Permit number: SDAUA-2014–011). The methods were carried out in accordance with the approved guidelines. Female mice, 8–10 weeks after birth, were intraperitoneally injected with 10 IU equine chorionic gonadotrophin (eCG). At 48 h after eCG injection, mice were sacrificed by decollation to collect ovaries for the recovery of oocytes. Only COCs with more than three layers of unexpanded CCs, containing oocytes larger than 70 μm in diameter and with a homogenous cytoplasm were used for experiments.

Preparation of oocytectomized cumulus oophorus complexes and denuded oocytes

To generate OOXs, the cytoplasm of each oocyte was microsurgically removed from the COCs using micromanipulators. The resulting OOXs consist of a hollow zona pellucida surrounded by several layers of intact CCs. To prepare DOs, CCs were mechanically removed from COCs by repeated passage of the COCs through a fine-bore fire-polished glass pipette in M2 medium.

Preparation of pig oocytes-conditioned medium

Porcine ovaries collected at a local slaughterhouse were transported to the laboratory within 3 h after slaughtering, in a thermos bottle with sterile saline containing 100 IU/ml penicillin and 0.05 mg/ml streptomycin, maintained at 30–35°C. COCs were recovered by aspirating 3–6 mm follicles using a syringe containing Dulbecco phosphate-buffered saline (D-PBS). Only COCs with a uniform

ooplasm and a compact cumulus were chosen for preparation of DOs. To prepare DOs, CCs were mechanically removed from COCs by repeated passage of the COCs through a fine-bore fire-polished glass pipette in D-PBS. To prepare POCM, 40 pig DOs were cultured for 36 h in 200 μl drops of a simplified α-minimum essential medium (s-MEM) medium (see below) at 39°C under humidified atmosphere with 5% CO_2 in air. At the end of the culture, POCM were recovered, centrifuged (200× *g*, 5 min) and stored at −20°C until use.

In vitro culture of cumulus-oocyte complexes or oocytectomized cumulus oophorus complexes

COCs and OOXs were cultured for 18 h in a s-MEM medium (about 30 COCs/OOXs per 100 μl drop) at 37.5°C under humidified atmosphere with 5% CO_2 in air. The s-MEM was formulated by removing all vitamins, amino acids (except glutamine), and nucleosides, and it thus contained inorganic salts (1.8 mM $CaCl_2$, 0.81 mM $MgSO_4$, 5.3 mM KCl, 26.2 mM $NaHCO_3$, 117.2 mM NaCl, 1.0 mM NaH_2PO_4), 2 mM glutamine, 5.56 mM glucose, 1 mM sodium pyruvate, 4 mg/ml bovine serum albumin (BSA), 0.03 mM phenol red, 50 IU/ml penicillin, and 50 μg/ml streptomycin.

To verify that OSFs inhibit CC apoptosis, OOXs were cocultured in s-MEM with mouse or pig DOs at different proportions. To study the effect of GDF-9 on CC apoptosis, mouse OOXs were cultured in s-MEM supplemented with various concentrations of recombinant mouse GDF-9 (Recombinant Mouse GDF-9, R&D Systems China Co. Ltd, Shanghai, China). GDF-9 was dissolved in 4 mM HCl containing 0.1% BSA to prepare a stock solution (100 μg/ml), which was stored at −20°C until use. To observe the roles of ALK5, SMAD3, and PI3K in regulating CC apoptosis, SB431542, a specific inhibitor of ALK 4/5/7, SIS3 (CAS1009104–85-1, Santa Cruz Biotechnology, Inc. Texas, USA) that selectively inhibits SMAD3 phosphorylation and its mediated cellular signaling, and LY294002 (L9908, Sigma), a PI3K inhibitor, were added at different concentrations to the s-MEM medium containing GDF-9 or to the POCM. The inhibitors were dissolved in dimethyl sulfoxide (DMSO) to make (20 mM) stock solutions, which was stored at −20°C until use.

Assessment of cell apoptosis

Cumulus cells released from about 30 OOXs or COCs were dispersed by repeatedly pipetting using a thin pipette. The dispersed cells were centrifuged (200× *g*) for 5 min at room temperature. The pellets were resuspended in 50 μl of M2 medium containing 0.01 mg/ml of Hoechst 33342 and stained in the dark for 5 min. The stained cells were resuspended in M2 medium and centrifuged at 200× *g* twice (5 min each). Finally, a 5 μl drop of suspension was smeared on a slide and examined under a Leica DMLB fluorescence microscope at a magnification of 400×. Six to eight fields were randomly observed on each smear. Cumulus cells in monolayer cultures were stained with Hoechst 33342 in situ in wells of a 96-well plate and observed under a fluorescence microscope. Four to five fields were randomly observed in each well. The heterochromatin was heavily stained and gave bright fluorescence. Whereas the apoptotic cells showed pyknotic nuclei full of heterochromatin, healthy cells showed normal nuclei with sparse heterochromatin spots (Figure 1A–C). To reduce the subjectivity, percentages of the apoptotic cells were always calculated double blindly by 2 investigators.

Quantitative real-time PCR

For Bcl-2, Bax, Drosha or Dicer, CCs from 50 OOXs or COCs from 2 mice, or CCs from 4 wells of monolayer culture in a 96-well plate, were used for total RNA isolation, which was performed using a RNAqueous-Micro Total RNA Isolation Kit (AM1931, Ambion, Austin, TX, USA). The RNA isolated was resuspended in diethyl pyrocarbonate (DEPC)-treated MilliQ water (DEPC-dH_2O). Reverse transcription was performed in a total volume of 20 μl using Transcriptor Reverse Transcriptase (03531287001, Roche, Basel, Switzerland). Briefly, 2 μl of each RNA sample was mixed in a 0.2 ml reaction tube with 1 μl Oligo dT18 (SO132, Fermentas, St. Leon-Rot, Germany), and 10 μl of DEPC-dH_2O, and the mixture was incubated in a PCR instrument at 65°C for 10 min. As soon as the incubation ended, the reaction tube was cooled on ice for 2 min and then centrifuged (200× *g*, 4°C) for a few seconds. Then, 4 μl of 5× RT buffer, 0.5 μl RNase inhibitor (03335402001, Roche, Basel, Switzerland), 2 μl dNTP (R0192, Fermentas, St. Leon-Rot, Germany) and 0.5 μl Transcriptor Reverse Transcriptase were added to the reaction tube. The mixture was then incubated at 55°C for 30 min, followed by incubation at 85°C for 5 min before storage at −20°C until use. Gene-specific primers for real-time RT-PCR are listed in Table 1. Quantification of mRNA was conducted using the Mx3005P real-time PCR instrument (Stratagene, Valencia, CA). Amplification reactions were performed in a 10 μl reaction volume containing 1 μl of cDNA, 5 μl of 2× SYBR Green Master Mix (600882, Agilent Technologies, Palo Alto, CA), 0.15 μl of ROX (reference dye), 3.25 μl of RNase-free water, and 0.3 μl each of forward and reverse gene-specific primers (10 μM). Cycle amplification conditions comprised an initial denaturation step at 95°C for 3 min followed by 40 cycles at 95°C for 20 s and 60°C for 20 s. Immediately after amplification, PCR products were analyzed by sequencing, dissociation curve analysis, and gel electrophoresis to determine specificity of the reaction. Gene expression was normalized to the glyceraldehyde 3-phosphate dehydrogenase (gapdh) internal control. All values were then expressed relative to the calibrator samples using the $2^{-(\Delta\Delta CT)}$ method.

For miR-21, CCs from about 240 OOXs or COCs from eight mice were used for total RNA isolation. Total RNA isolation was performed using a mirVana miRNA Isolation Kit (AM1561, Ambion, Austin, TX, USA). The RNA isolated was resuspended in DEPC-dH_2O. For miRNA stem-loop reverse transcription, 2 μl total RNA and 9 μl RNase-free H_2O were mixed and heated at 65°C for 10 min followed by quenching on ice. Then, 4 μl 5× RT buffer, 0.5 μl RNase inhibitor (03335402001, Roche, Basel, Switzerland), 2 μl 10 mM dNTP (R0192, Fermentas, St. Leon-Rot, Germany), 2 μl 10 μM stem-loop reverse transcription primer (Table 1), and 0.5 μl reverse transcriptase (03531287001, Roche, Basel, Switzerland) were added and mixed to set up 20 μl reactions. The 20 μl reactions were incubated in Mastercycler (Eppendorf) for 30 min at 55°C, 5 min at 85°C, and held at 4°C. Reactions for real time-quantitative PCR (RT-qPCR) including negative control were performed in triplicate. For RT-qPCR, the reaction mixture was prepared according to the manufacturer's instructions with Brilliant III Ultra-Fast QPCR Master Mix (600880, Agilent Technologies, Palo Alto, CA, USA). The concentration of primers and Taqman probes was optimized and verified by standard curve. The concentration of forward and reverse primer was 600 and 300 nM, respectively. The concentration of Taqman probes was 200 nM for U6 and mmu-miR-21. The sequences of primers and Taqman probes used were listed in Table 1. Reactions were run in Mx3005P (Stratagene) as follows: 95°C

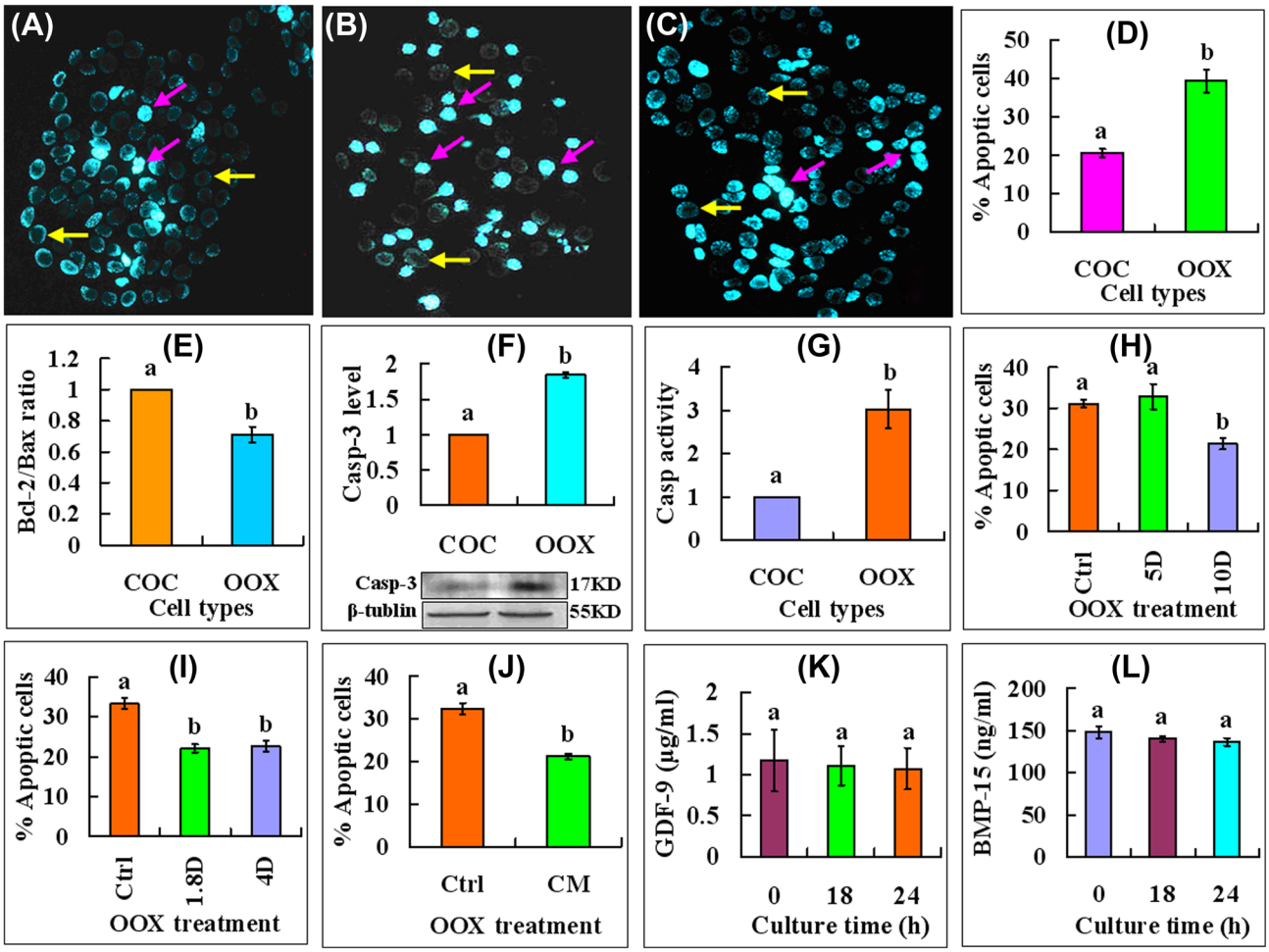

Figure 1. Apoptosis of CCs after culture of mouse COCs or OOXs alone or with mouse or pig DOs. Micrographs A, B, and C show CC smears stained with Hoechst 33342 and observed under a fluorescence microscope. The heterochromatin was heavily stained with Hoechst and gave bright fluorescence. Whereas the apoptotic cells showed pyknotic nuclei full of heterochromatin (pink arrows), healthy cells showed normal nuclei with sparse heterochromatin spots (yellow arrows). Smears A and B show CCs from COCs and OOXs, respectively, whereas C shows CCs from OOXs cultured with mouse DOs at a 1:5 ratio. Original magnification ×400. Graphs D–G show percentages of apoptotic cells, Bcl-2/Bax ratio (real-time PCR results), relative levels of active caspase-3 expression (western blot analysis), and relative caspase-3 activities, respectively, in CCs from mouse COCs and OOXs cultured alone. Graphs H and I show percentages of apoptotic CCs following culture of mouse OOXs alone (Ctrl) or with mouse DOs at 1:5 (5D) or 1:10 (10D) ratio (graph H) or with pig DOs at 1:1.8 (1.8D) or 1:4 (4D) ratio (graph I). Graph J shows percentages of apoptotic cells after culture of mouse OOXs in s-MEM (Ctrl) or in pig oocyte-conditioned medium (CM). Graphs K and L show concentrations of GDF-9 (μg/ml) and BMP-15 (ng/ml) in POCM after culture of mouse OOXs for different times. For assessment of percentages of apoptotic cells, each treatment was repeated six times with each replicate including one smear of about 30 OOXs. For RT-PCR and western analysis, the relative quantity value of Bcl-2/Bax or active caspase-3 in COCs was set as 1, and other values were expressed relative to this quantity. a, b: values with a different letter above their bars differ significantly ($P < 0.05$).

for 3 min followed by 40 cycles of 95°C for 20 s and 58°C for 20 s. The FAM and ROX fluorescence were collected after each cycle. Relative expression of miR-21 was calculated by MxPro software with $2^{-(\Delta\Delta CT)}$ and U6 as normalizer.

Western blotting

Cumulus cells from 250–300 OOXs or COCs from 10 mice, or CCs from 10 wells of monolayer culture in a 96-well plate, were placed in a 1.5 ml microfuge tube containing 20 μl sample buffer (20 mM Hepes, 100 mM KCl, 5 mM $MgCl_2$, 2 mM DTT, 0.3 mM phenylmethyl sulfonyl fluoride, 3 μg/ml leupetin, pH 7.5) and frozen at −80°C. To run the gel, 5 μl of 5× sodium dodecyl sulphate - polyacrylamide gel electrophoresis (SDS-PAGE) loading buffer was added to each tube, and the tubes were heated to 100°C for 5 min. Total proteins were separated on a 15% polyacrylamide gel by SDS-PAGE and transferred electrophoretically onto PVDF membranes. After being washed in Tris-buffered saline with Tween 20 (TBST) (150 mM NaCl, 2 mM KCl, 25 mM Tris, 0.05% Tween 20, pH 7.4) and blocked with TBST containing 3% BSA for 1 h at 37°C, the membranes were incubated at 4°C overnight with rabbit antiactive caspase-3 polyclonal antibodies (1:1000, ab13847, Abcam Co. Ltd) and mouse anti-β-tubulin monoclonal antibodies (1:1000, 05-661, Merck Millipore). Then, the membranes were washed in TBST and incubated for 1 h at 37°C with alkaline phosphatase-conjugated goat antirabbit IgG (1:1000, cw0111, Kangweishiji Biotechnology Co. Ltd, Beijing, China) and goat antimouse IgG (1:1000, cw0110, Kangweishiji Biotechnology Co. Ltd, Beijing, China). Finally, signals were detected by a BCIP/NBT alkaline phosphatase color

Table 1. Sequences of stem-loop primers, RT-PCR primers and Taqman probes used in this study.

Gene	Oligonucleotide sequences
Stem-loop primers	
U6	5′-AACGCTTCACGAATTTGCGT-3′
mmu-miR-21	5′-CTCAACTGGTGTCGTGGAGTCGGCAATTCAGTTGAGTCAACATC-3′
RT-PCR primers	
U6	F: CTCGCTTCGGCAGCACA
	R: AACGCTTCACGAATTTGCGT
	P: 5′-FAM-AGATTAGCATGGCCCCTGCGCAA-BHQ-3′
mmu-miR-21	F: ACACTCCAGCTGGGTAGCTTATCAGACTGA
	R: TGGTGTCGTGGAGTCG
	P: 5′ FAM-TTCAGTTGAGTCAACATC-3′ BHQ
Bcl2	F: TTCGGGATGGAGTAAACTGG
	R: TGGATCCAAGGCTCTAGGTG
Bax	F: TGCAGAGGATGATTGCTGAC
	R: TGGATCCAAGGCTCTAGGTG
Drosha	F: ATGCAAGGCAATACGTGTCAT
	R: TTTTGGGGTCTGAAAGCTGGT
Dicer	F: GGTCCTTTCTTTGGACTGCCA
	R: GCGATGAACGTCTTCCCTGA
Has2	F: GAGCACCAAGGTTCTGCTTC
	R: CTCTCCATACGGCGAGAGTC
Gapdh	F: AAGGTGGTGAAGCAGGCAT
	R: GGTCCAGGGTTTCTTACTCCT

F: forward; R: reverse; P: Taqman probe.

development kit (Beyotime Institute of Biotechnology, Haimen City, China). The relative quantities of proteins were determined with Image J software by analyzing the sum density of each protein band image.

Caspase-3 activity assays

Caspase-3 activity was determined by using a Caspase-3 Activity Assay Kit (Beyotime Institute of Biotechnology, China). Briefly, CCs from 100 COCs/OOXs were harvested and washed twice in cool PBS. Then, the CCs were lysed with 50 μl lysis buffer for 15 min on ice, and the lysate was centrifuged at 600× *g* for 5 min at 4°C. After that, the supernatant was collected and frozen at −80°C. To measure caspase-3 activity, 50 μl of supernatant, 40 μl of reaction buffer and 10 μl of 2 mM caspase-3 substrate Ac-DEVD-pNA (acetyl-Asp-Glu-Val-Aspp-nitroani lide) were mixed in well of a 96-well plate and incubated at 37°C overnight. The absorbance of the yellowish p-nitroanilide was determined at 405 nm using a microplate reader (BioTek-ELx808, BioTek Instruments, Inc.).

Enzyme-Linked Immunosorbent Assay (ELISA) of growth differentiation factor-9 and bone morphogenetic protein-15 in pig oocyte-conditioned medium

Mouse OOXs were cultured in POCM for 0, 18, or 24 h before POCM recovery for ELISA detection for GDF-9 and BMP-15. ELISA of POCM was performed using ELISA kits for porcine GDF-9 or BMP-15 (BLUE GENE, Shanghai, China). Briefly, 100 μl of standards or POCM were added to the well in the antibody precoated microtiter plate, and 100 μl of PBS (pH 7.0–7.2) was placed in the blank control well. Then, 10 μl of balance solution (not for standards) and 50 μl of conjugate were added to each well. The plate was then incubated for 1 h at 37°C. After that, 50-μl substrate A and 50-μl substrate B were added to each well, and the plate was incubated for 10–15 min at 20–25°. Finally, 50 μl of stop solution was added to each well, and the OD values were read at 450 nm using a microplate reader (BioTek-ELx808, BioTek Instruments, Inc.). The GDF-9 and BMP-15 concentrations were calculated according to their respective standard curves.

Cumulus cell culture and transfection

Knockdown or overexpression of miR-21 was conducted by transfection of CC monolayers with miRNA inhibitor or mimic, respectively. To establish the CC monolayer culture, freshly recovered COCs were repeatedly pipetted in M2 medium using a fine-bore fire-polished glass to release CCs. The CCs recovered were washed in the DMEM medium, counted on a hemocytometer, seeded in wells of a 96-well plate (1.5−2 × 10^4 CCs/well), and then, cultured at 37.5°C in a humidified atmosphere of 5% CO_2 in air. The DMEM medium (11330032, Invitrogen, Carlsbad, CA, USA) was supplemented with 10% fetal bovine serum, 50 IU/ml penicillin, and 50 μg/ml streptomycin. At 48 h after seeding when monolayers were formed (90% confluent), transfection of miR-21 mimic or inhibitor or their control was performed (Supplementary Figure S1A).

The miR-21 mimic (5′-AACAUCAGUCUGAUAAGCUAUU-3′), miR-21 inhibitor (5′- UCAACAUCAGUCUGAUAAGCUA-3′), and their negative control were synthesized by Ribobio Co., Ltd, Guangzhou, Guangdong, China. The oligonucleotides of miR-21 mimic and miR-21 inhibitor were transfected at a final concentration of 50 and 100 nM, respectively. To prepare a 100 mM stock solution, the oligonucleotides were dissolved in DEPC-dH_2O, and the stock solution was stored at −20°C until use. MicroRNA-21 mimic or inhibitor or their control were transfected by adding to each culture well 0.75 μl of Lipofectamine RNAiMAX Reagent (13778500, Invitrogen, Carlsbad, CA, USA), 25 μl Opti-MEM I Reduced Serum Medium (51985042, Life technologies, Gaithersburg, MD, USA), 10 μl of miRNA-lipid complex, and 90 μl DMEM medium. At 48 h after the transfection, the transfection mix was replaced with s-MEM, and the cells were cultured for 24 or 48 h (Supplementary Figure S1A). To serve as controls, some confluent CCs were

cultured continuously for 96 h in DMEM without transfection, and the nontransfected CCs were also cultured in s-MEM medium for 24 or 48 h. At the end of the culture, some CCs were immediately stained with Hoechst 33342 and examined for apoptosis, whereas others were digested for 2 min at 37.5°C with 0.25% trypsin and washed twice by centrifugation (200× *g* for 5 min) in DMEM containing 10% fetal bovine serum. Then, the resulting cell suspension was used for real-time PCR, western blotting or caspase-3 activity assays.

To test whether our monolayer culture of oocytes-separated CCs would retain their function similar to that in a three-dimensional COC, their response to follicle-stimulating hormone (FSH) and GDF-9 was examined at different times of culture. Cumulus cells were first cultured for 48 or 96 h in DMEM before a test culture in TCM-199 for 24 h with or without FSH in the presence of GDF-9. At the end of the test culture, mRNA levels of the cumulus-expansion-related hyaluronan synthase 2 (HAS2) [32] were analyzed by real-time PCR. Whether CCs were cultured in DMEM for 48 or 96 h, the presence of FSH during test culture significantly increased the level of HAS2 mRNA to a level similar to that in COCs cultured with FSH, although the presence of GDF-9 showed no significant effect (Supplementary Figure S1B). Furthermore, our experiments on the effects of up- or downregulating the expression of miR-21 on CC apoptosis indicated that after control CCs were cultured in DMEM for 96 h, the presence of GDF-9 during the test culture significantly reduced CC apoptosis with decreased levels of active caspase-3 and caspase-3 activities (see below in the Results and Discussion sections). It has been reported that miR-26b triggered apoptosis in porcine granulosa cells by downregulating HAS2, while upregulating caspase-3 expression [33]. Together, the data suggested that CCs retained their basic functions after our monolayer culture for over 96 h.

Data analysis

There were at least three replicates for each treatment unless otherwise stated. Percentage data were arc sine transformed, and analyzed with ANOVA when each measure contained more than two groups or with independent-sample *t*-test when each measure had only two groups; a Duncan multiple comparison test was used to locate differences. The software used was Statistics Package for Social Sciences (SPSS 11.5, SPSS Inc. Chicago, IL, USA). Data were expressed as mean ± SEM and $P < 0.05$ were considered significant.

Results

Mouse and pig oocytes inhibited in vitro apoptosis of mouse cumulus cells by producing soluble factors

Four experiments were conducted to confirm that oocytes inhibit apoptosis of mouse CCs by producing soluble factors. In the first experiment, levels of CC apoptosis were compared between mouse COCs and OOXs after culture in s-MEM medium. While the percentage of apoptotic cells, the level of active caspase-3, and the caspase-3 activity in CCs were higher, the Bcl-2/Bax ratio was lower significantly in OOXs than in COCs (Figure 1D–G), confirming the antiapoptotic role for oocytes. In the second experiment, mouse OOXs were cocultured with mouse or pig DOs at different proportions to observe the effect of oocyte-derived soluble factors on CC apoptosis. Although coculture of OOXs with mouse DOs at a 1:5 ratio showed no effect, culture at a 1:10 ratio significantly reduced the apoptotic cell percentage of the OOXs (Figure 1H). Coculture of mouse OOXs with pig DOs at either 1:2 or 1:4 ratio significantly reduced CC apoptosis (Figure 1I). The third experiment showed that the percentage of apoptotic cells decreased significantly when mouse OOXs were cultured in POCM (Figure 1J). In the fourth experiment, concentrations of GDF-9 and BMP-15 in POCM were measured by ELISA at different times during culture of mouse OOXs. The results showed that concentrations of GDF-9 (1.17 ± 0.38, 1.11 ± 0.24 and 1.07 ± 0.25 μg/ml at 0, 18, and 24 h of culture, respectively) and BMP-15 (148.03 ± 7.04, 140.08 ± 3.73 and 136.68 ± 4.44 ng/ml at 0, 18 and 24 h of culture, respectively) in POCM did not change significantly during the culture (Figure 1K and L), suggesting that GDF9 and BMP-15 are secreted and stable in oocyte-conditioned media. Taken together, the results suggest that mouse and pig oocytes inhibited mouse CC apoptosis by producing soluble factors including GDF-9 and BMP-15.

Culture of mouse oocytectomized cumulus oophorus complexes with recombinant mouse growth differentiation factor-9 suppressed cumulus cell apoptosis

To answer the question whether oocytes suppress CC apoptosis by secreting GDF-9, mouse OOXs were cultured in s-MEM with various concentrations of recombinant GDF-9 before examination for CC apoptosis. The results showed that GDF-9 significantly decreased apoptosis levels of OOXs in a dose-dependent manner, and the percentage of apoptotic CCs reached a level similar to that in cultured COCs (around 20%; Figure 1D) by 1 μg/ml (Figure 2A). Furthermore, culture of OOXs with GDF-9 significantly increased the Bcl-2/Bax ratio (Figure 2B) while decreasing the level of active caspase-3 (Figure 2C) to levels similar to those observed in COCs cultured without GDF-9. The results suggest that oocytes inhibited CC apoptosis by producing GDF-9.

The GDF-9 concentration (1 μg/ml) we found effective to inhibit CC apoptosis was much higher than those reported by Dragovic et al. [34] who used 145 ng/ml of GDF9 to promote cumulus expansion of mouse OOXs in the presence of both serum and FSH, by Lin et al. [35] who used 100 ng/ml of GDF-9 to facilitate cumulus expansion of pig COCs in the presence of eCG and hCG, and by Gilchrist et al. [36] who used 60 ng/ml GDF-9 to promote mouse granulosa cell proliferation in the presence of DOs. These previous studies suggested that the presence of either serum plus FSH or DOs that could secrete OSFs might have sensitized CCs to lower doses of GDF9. Because the s-MEM medium we used to culture mouse OOXs did not contain any serum, hormone, or DOs, we tested whether the involvement of serum, gonadotropin, and/or multiple OSFs could reduce the dosage of GDF-9. Mouse OOXs were cultured with a lower concentration (250 ng/ml) of GDF-9 in the presence of serum, FSH, or BMP-15 before examination for CC apoptosis. The results showed that culture of OOXs with either serum, BMP-15, or particularly serum plus FSH, significantly decreased the percentage of apoptotic CCs compared to that in OOXs cultured with GDF-9 alone (Figure 2D). The results suggested a synergetic effect among OSFs, serum, and gonadotropin. Wang et al. [27] have incubated pig OOXs with 1 μg/ml of GDF-9 in MEM without serum or hormone supplementation to determine whether GDF-9 activates PI3K pathways.

Oocyte-secreted factors and recombinant growth differentiation factor-9 inhibited cumulus cell apoptosis through activation of ALK5 and SMAD3

To study whether OSFs and GDF-9 inhibit CC apoptosis by activating ALK5 and SMAD3, we observed the effects of ALK5 inhibitor

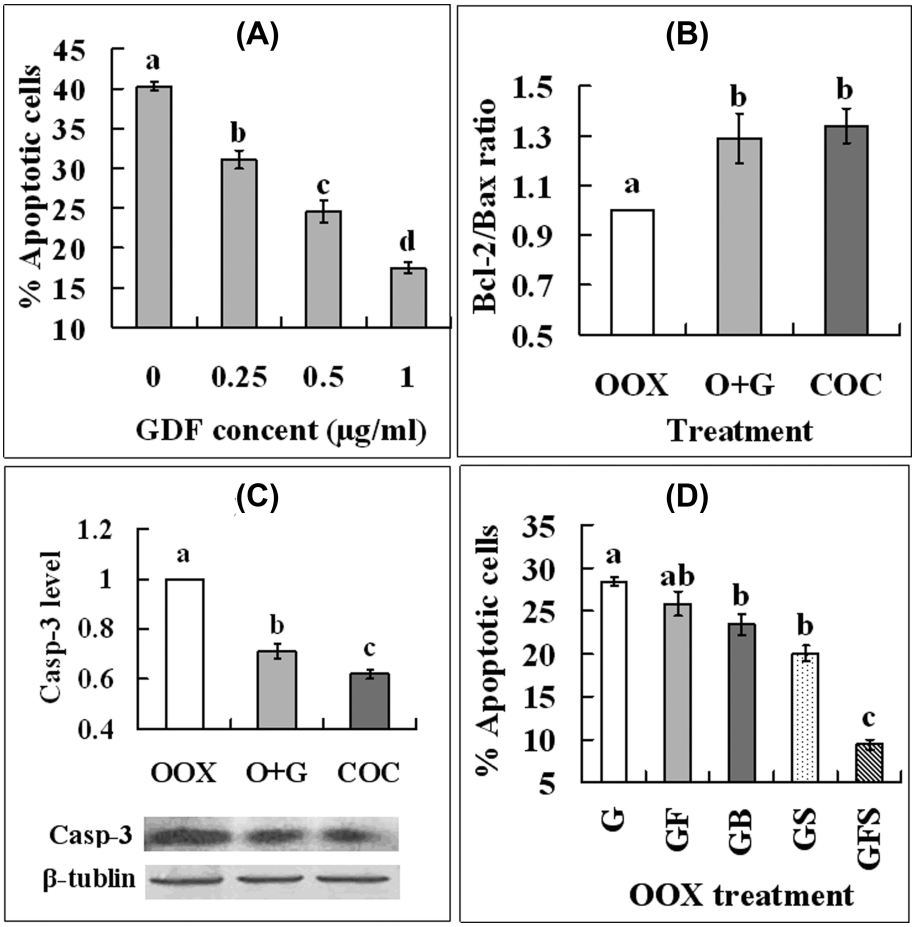

Figure 2. Effects of culture with recombinant GDF-9 on CC apoptosis of mouse OOXs. In graph A, mouse OOXs were cultured for 18 h in s-MEM with various concentrations of GDF-9 before examination for apoptotic percentages of CCs. Each treatment was repeated six times with each replicate including one smear of about 30 OOXs. In graphs B and C, OOXs or COCs were cultured in s-MEM alone or with 1 μg/ml GDF-9 (O+G) before real-time PCR analysis for Bcl-2 and Bax mRNA expression or western blot analysis for active caspase-3 levels, respectively. The quantity value of Bcl-2/Bax or active caspase-3 in control OOXs cultured in s-MEM alone was set as 1, and other values were expressed relative to this quantity. In graph D, mouse OOXs were cultured for 18 h in s-MEM with 250 ng/ml of GDF-9 alone (G) or with 0.5 μg/ml of FSH (GF), 250 ng/ml BMP-15 (GB), 10% serum (GS), or FSH and serum (GFS), before examination for apoptotic percentages of CCs. Each treatment was repeated three times with each replicate including one smear of about 30 OOXs. a–d: values with a different letter above bars differ significantly ($P < 0.05$).

(SB431542) and SMAD3 inhibitor (SIS3) on CC apoptosis during culture of mouse OOXs with recombinant GDF-9 or in POCM. To determine the optimal concentration of SB431542 and SIS3, COCs were cultured for 18 h in s-MEM containing different concentrations of the drugs before examination for CC apoptosis. The results showed that 100 μM of SB431542 (Figure 3A) and 5 μM of SIS3 (Figure 3B) were the optimal concentrations that increased apoptotic rates of CCs to a level similar to that observed after culture of OOXs without GDF-9 (around 35%; Figure 1D). When OOXs were cultured with GDF-9, the presence of either SB431542 or SIS3 significantly increased CC apoptosis (Figure 3C) and active caspase-3 expression (Figure 3D), while decreasing the ratio of Bcl-2/Bax (Figure 3E) to levels similar to those observed in control OOXs cultured alone. When OOXs were cultured without GDF-9, however, neither 100 μM of SB431542 (32.8 ± 1.2% versus 33.1 ± 1.1%) nor 5 μM of SIS3 (31.3 ± 1.2% versus 31.8 ± 1.5%) affected CC apoptotic rates, suggesting that both SB431542 and SIS3 are nontoxic to mouse CCs when used at the selected concentrations. Furthermore, when mouse OOXs were cultured in POCM, the presence of either SB431542 or SIS3 significantly increased CC apoptosis (Figure 3F).

Recombinant growth differentiation factor-9 and pig oocyte-conditioned medium upregulated microRNA-21 expression in cumulus cells with activation of the TGF-β superfamily signaling pathway

COCs or OOXs were cultured for 18 h in s-MEM alone or with GDF-9 with or without SB431542 or SIS3 before examination for levels of miR-21 expression in CCs. The results show that the relative level of miR-21 was significantly lower in OOXs than in COCs after culture in s-MEM alone, but miR-21 level increased significantly when OOXs were cultured in the presence of GDF-9 (Figure 4A). The presence of SB431542 or SIS3 completely abolished the beneficial effect of GDF-9 on miR-21 expression. Similarly, culture of mouse OOXs in POCM significantly increased the level of miR-21 in CCs, and the addition of either SB431542 or SIS3 eliminated the beneficial effect of POCM (Figure 4B). Together, the results suggest that oocyte-derived growth factors including GDF-9 inhibited CC apoptosis with upregulation of miR-21 expression, and that it upregulated miR-21 expression with activation of the TGF-β superfamily signaling pathway.

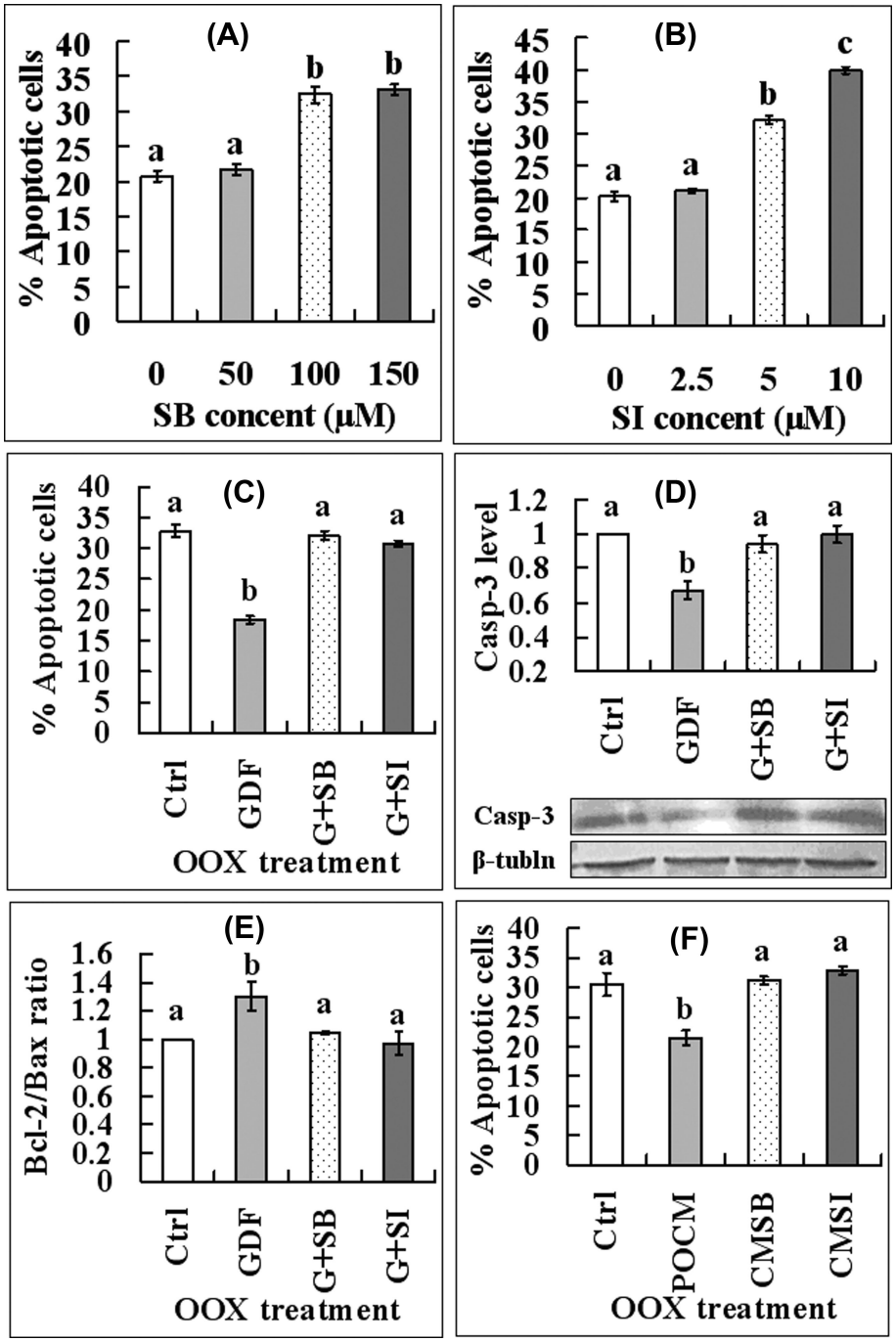

Figure 3. Effects of inhibiting ALK5 or SMAD3 on the antiapoptotic effect of GDF-9. In graphs A and B, mouse COCs were cultured for 18 h in s-MEM with different concentrations of ALK5 inhibitor, SB431542 (SB) or SMAD3 inhibitor, SIS3 (SI) before examination for apoptotic percentages of CCs. In graphs C–E, mouse OOXs were cultured for 18 h in s-MEM alone (Ctrl) or with 1 μg/ml GDF-9 (GDF) without or with 100-μM SB (G+SB) or 5-μM SI (G+SI) before examination for CC apoptosis, western blot analysis for active caspase-3 expression or real-time PCR for Bcl-2 and Bax mRNAs. In graph F, mouse OOXs were cultured for 18 h in s-MEM alone (Ctrl) or in pig oocytes-conditioned medium (POCM) without or with SB (CMSB) or SI (CMSI) before examination for CC apoptosis. For examination of CC apoptosis, each treatment was repeated six times with each replicate including one smear of about 30 COCs or OOXs. For RT-PCR and western analysis, the relative quantity value of Bcl-2/Bax or active caspase-3 in control OOXs cultured in s-MEM alone was set as 1, and other values were expressed relative to this quantity. a–c: values with a different letter above bars differ significantly ($P < 0.05$).

To study whether the OSF upregulation of miR-21 expression is associated with an increase in DROSHA and/or DICER, levels of miR-21 and of Drosha and Dicer1 mRNAs were analyzed by real-time PCR using the same samples. While COCs were cultured in s-MEM, OOXs were cultured in s-MEM or POCM for 18 h before a simultaneous measurement for levels of both miR-21 and Drosha/Dicer1 mRNAs in CCs. Although the level of Dicer1 mRNA was closely correlated with that of miR-21, the level of Drosha

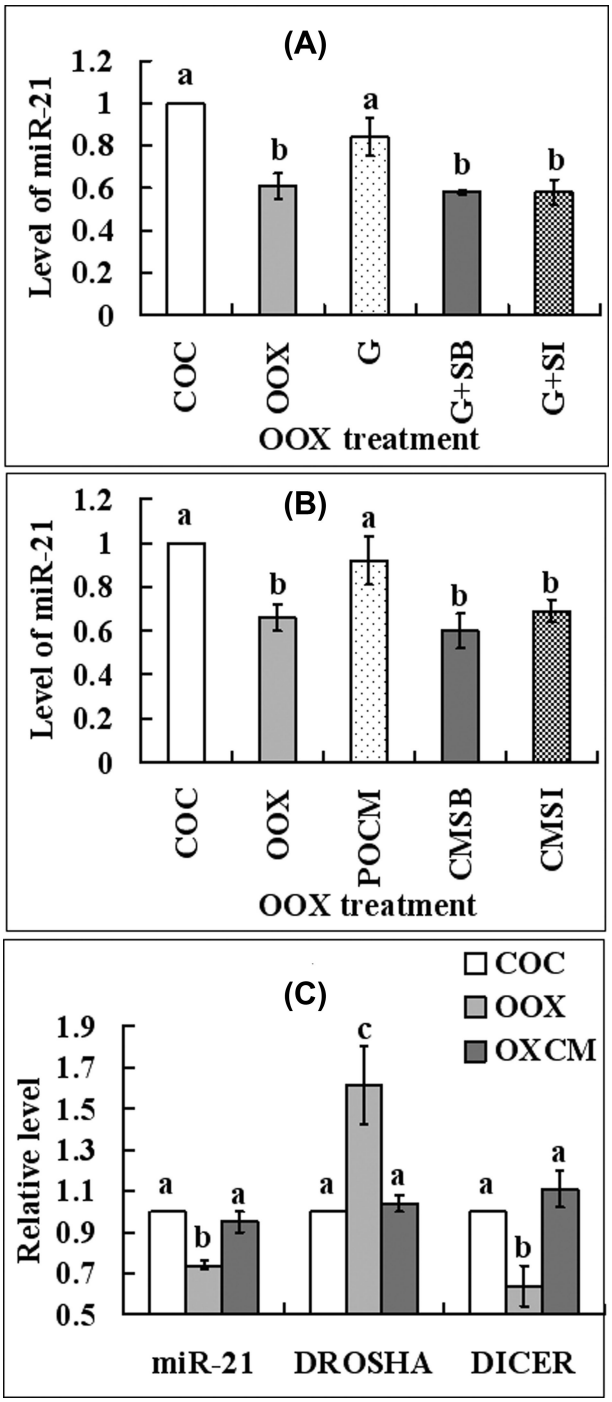

Figure 4. Relative levels of miR-21 and Drosha/Dicer1 mRNAs in CCs after culture of mouse COCs or OOXs with GDF-9 or in POCM in the presence or absence of ALK5 inhibitor, SB431542 (SB) or SMAD3 inhibitor, SIS3 (SI). (A) Mouse COCs or OOXs were cultured for 18 h in s-MEM alone or with 1 μg/ml GDF-9 (G) without or with 100-μM SB or 5-μM SI. (B) Mouse COCs or OOXs were cultured for 18 h in s-MEM alone or in POCM without or with SB (CMSB) or SI (CMSI). Each treatment was repeated three times and each replicate contained CCs from about 240 COCs or OOXs. (C) While COCs were in s-MEM (COC), OOXs were cultured in s-MEM (OOX) or POCM (OXCM) for 18 h before real-time PCR measurement for Drosha or Dicer1 mRNA levels. The relative quantity values of miR-21 or Drosha/Dicer1 mRNA in COCs cultured in s-MEM alone were set as 1, and other values were expressed relative to this quantity. a, b: Values with a different letter above bars differ significantly ($P < 0.05$).

mRNA was significantly lower in COCs cultured in s-MEM and in OOXs cultured in POCM than that in OOXs cultured in s-MEM (Figure 4C). The results suggested that OSFs promoted miR-21 processing in CCs through DICER but not through DROSHA.

Effects of up- or downregulating microRNA-21 expression on cumulus cell apoptosis

Cumulus cell monolayers were transfected with miR-21 mimic or inhibitor (anti-miR-21) by Lipofectamine before culture for 24 h in s-MEM with or without GDF-9 supplementation. At the end of the post-transfection culture, CCs were examined for apoptotic percentages, active caspase-3 levels, caspase-3 activities, and Bcl2/Bax ratios. When the post-transfection culture was conducted in s-MEM without GDF-9, transfection of miR-21 mimic reduced the apoptotic percentage, the active caspase-3 level and caspase-3 activity while increasing the Bcl-2/Bax ratio significantly, although transfection of miR-21 inhibitor showed no significant effect on these parameters of CCs (Figure 5). When post-transfection culture was conducted in the presence of GDF-9, however, transfection of miR-21 inhibitor increased the apoptotic percentage, active caspase-3 level, and caspase-3 activities while decreasing the Bcl-2/Bax ratio of CCs significantly. Furthermore, when the post-transfection culture was extended to 48 h, the difference in apoptotic percentages of CCs became even more pronounced among different treatments (Figure 5E). Taken together, the results suggest that GDF-9 inhibited CC apoptosis by upregulating miR-21.

To explore the question why transfection of miR-21 inhibitor had no effect on apoptosis of CC monolayers cultured without OSFs, we compared apoptosis and miR-21 levels between OOXs and CC monolayers cultured in s-MEM or POCM. While OOXs were cultured for 18 h, CC monolayers were cultured for 48 h before assays. The results showed that culture in POCM significantly increased levels of miR-21 (Figure 5F) while decreasing percentages of apoptotic cells (Figure 5G) in both CC monolayers and OOXs. Cumulus cell monolayers contained two to three folds more miR-21 than OOXs did after culture in either s-MEM or POCM. While the results further explained why CCs were significantly less apoptotic after culture of CC monolayers than after culture of OOXs, they refuted our expectation that the inability of miR-21 inhibitors to increase apoptosis of CC monolayers cultured without OSFs was because CC monolayers contain much less miR-21 than OOXs do after culture without OSFs. Thus, the question why transfection of miR-21 inhibitors did not affect apoptosis of CC monolayers cultured without OSFs remains to be answered.

Role of the PI3K/Akt signaling in mediating microRNA-21 inhibition on cumulus cell apoptosis

To study the mechanism by which the OSF-upregulated miR-21 inhibits CC apoptosis, three experiments were carried out in which the PI3K/Akt pathway was inhibited with PI3K inhibitor, LY294002. In the first experiment, mouse COCs were cultured for 18 h in s-MEM with different concentrations of PI3K inhibitor, LY294002 before examination for CC apoptosis. The percentage of apoptotic cells increased with increasing LY294002 concentrations, and at 20 μM of LY294002, it reached 32% (Figure 6A), a level similar to that observed in OOXs cultured in s-MEM alone. In the second experiment, mouse OOXs were cultured for 18 h in s-MEM alone, or in the presence of recombinant GDF-9 with or without 20-μM LY294002, before CC apoptosis evaluation. The results showed that in the presence of GDF-9, LY294002 significantly increased CC apoptosis to a

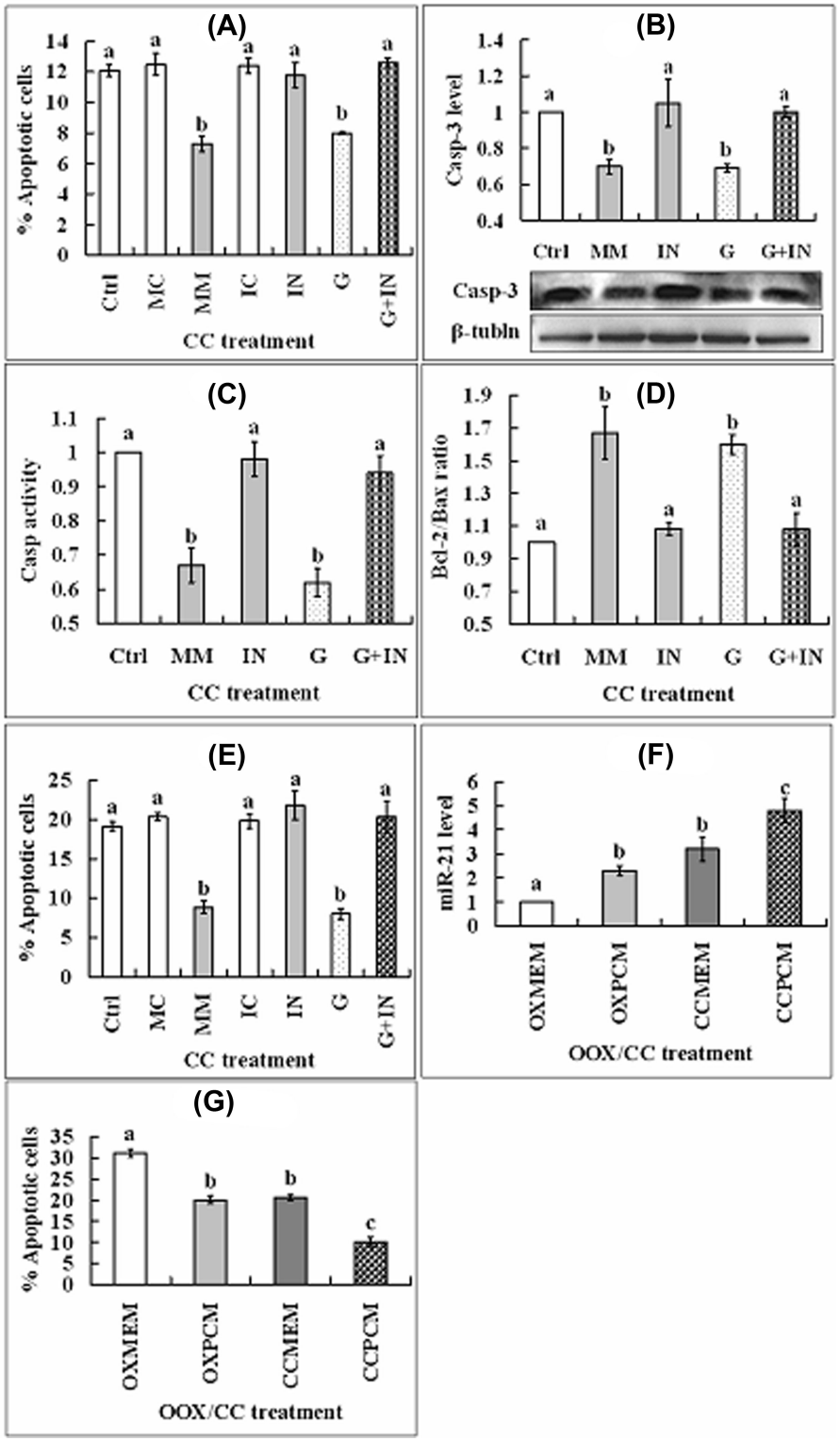

Figure 5. Effects of up- or downregulating the expression of miR-21 on CC apoptosis. Cumulus cell monolayers were transfected with miR-21 mimic (MM) or mimic control (MC), or with miR-21 inhibitor (IN) or inhibitor control (IC) before culture for 24 h with or without 1 μg/ml GDF-9 (G) supplementation. Nontransfected CCs were also cultured in simplified s-MEM medium for 24 h to serve as controls (Ctrl). At the end of the culture, CCs were examined for apoptotic percentages (Panel A), levels of active caspase-3 (Panel B), caspase-3 activity (Panel C), or Bcl2/Bax ratio (Panel D). Panel E shows the apoptotic percentages of CCs after the post-transfection culture was extended to 48 h. Panels F and G show miR-21 levels and percentages of apoptotic CCs, respectively, after culture in s-MEM or POCM of OOXs for 18 h (OXMEM or OXPCM) or of CC monolayers for 48 h (CCMEM or CCPCM). For examination of CC apoptosis, each treatment was repeated six times with each replicate including one culture well of monolayer CCs. For RT-PCR, western analysis and caspase-3 activity assay, the relative quantity value of Bcl-2/Bax, active caspase-3, or caspase-3 activity in control CCs cultured in s-MEM alone was set as 1, and other values were expressed relative to this quantity. a–c: values with a different letter above bars differ significantly ($P < 0.05$).

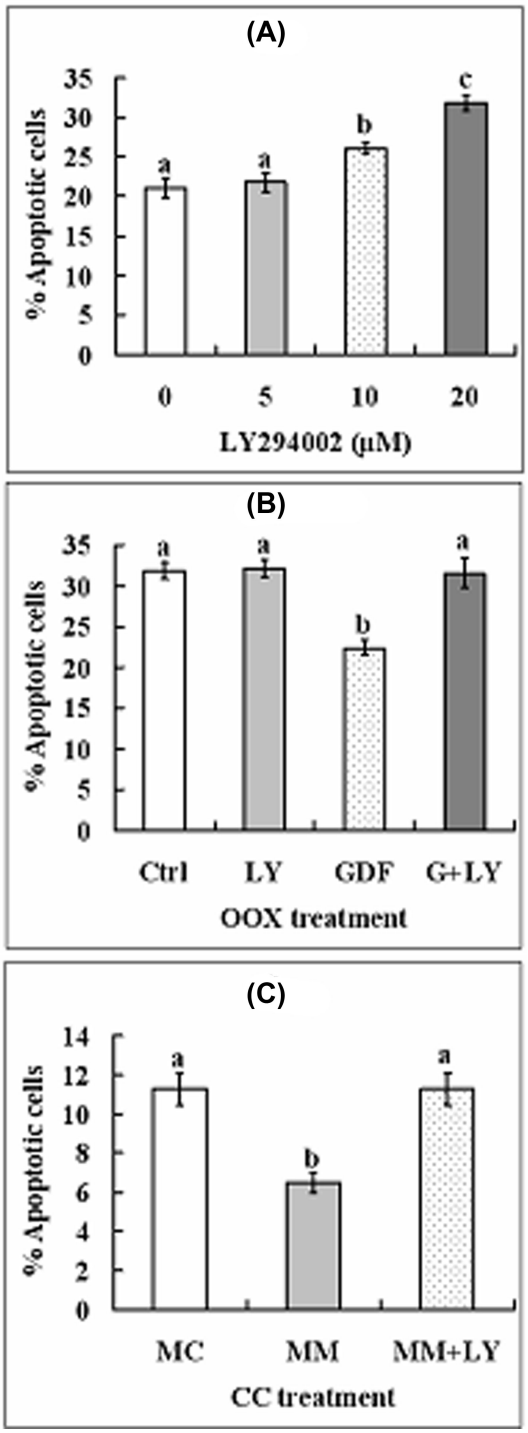

Figure 6. Effects of inhibiting the PI3K/Akt signaling with LY294002 on CC apoptosis. (A) Mouse COCs were cultured for 18 h in s-MEM with different concentrations of PI3K inhibitor, LY294002 before examination for apoptotic percentages of CCs. Each treatment was repeated six times with each replicate including one smear of about 30 COCs. (B) Mouse OOXs were cultured for 18 h in the simplified s-MEM alone (Ctrl), or in the presence of 1 μg/ml recombinant GDF-9 with or without 20-μM LY294002 (LY), before CC apoptosis evaluation. Each treatment was repeated six times with each replicate including one smear of about 30 OOXs. C. Mouse CCs that had been transfected with miR-21 mimic control (MC) or mimic (MM) were cultured for 24 h with or without 20-μM LY before CC apoptosis evaluation. Each treatment was repeated six times with each replicate including one culture well of monolayer CCs. a, b: values with a different letter above bars differ significantly ($P < 0.05$).

level similar to that in OOXs cultured in s-MEM alone (Figure 6B). When OOXs were cultured without GDF-9, however, LY294002 showed no effect on CC apoptosis, suggesting that LY294002 is nontoxic to mouse CCs when used at the selected concentration. In the third experiment, CC monolayers that had been transfected with miR-21 mimic (MM) or mimic control (MC) were cultured for 24 h with or without LY294002 before CC apoptosis evaluation. The results showed that the presence of LY294002 significantly increased apoptosis in the CCs transfected with MM to a level similar to that when the CC monolayers transfected with MC were cultured without LY294002 (Figure 6C). Taken together, the results suggest that the OSF-upregulated miR-21 inhibits CC apoptosis by activating the PI3K/Akt signaling.

Discussion

Because recombinant GDF-9 and BMP-15 preparations may not represent the native forms secreted by oocytes [15], and may generate artifacts in vitro when nonhomologous recombinant preparations are used [37], we adopted both in vitro treatments of mouse OOXs with recombinant mouse GDF-9 and bioassays with native OSFs (coculture with mouse or pig DOs or culture in POCM) to explore the mechanisms by which oocytes inhibit CC apoptosis. The results show that either coculture with mouse or pig DOs or culture with recombinant mouse GDF-9 or in POCM significantly suppressed CC apoptosis of mouse OOXs, suggesting that mouse oocytes inhibited CC apoptosis by secreting OSFs including GDF-9. In rats, GDF-9 antisense activated caspase-3 and induced apoptosis in cultured preantral follicles, and the response was attenuated by treatment with exogenous GDF-9 [38]. In bovine, CC apoptosis was significantly reduced by BMP-15, whereas GDF-9 showed no significant effect on CC apoptosis [9]. In pigs, the apoptotic level of CCs decreased significantly following treatment with GDF-9 [27] or BMP-15 [39].

There are several reports that mouse oocytes express Gdf-9 and Bmp-15 mRNAs. For example, GDF-9 mRNA was detected in mouse oocytes at all stages of follicular development and after ovulation [12]. A combination of northern blot and in situ hybridization analyses demonstrated that mouse Bmp-15 mRNA was expressed specifically in the oocyte beginning at the one-layer primary follicle stage and continuing through ovulation [40]. However, recent studies have shown that the functional mature form of BMP-15 is barely detectable in the mouse oocytes until just before ovulation [41], and that while human and ovine BMP-15 and mouse, human, and ovine GDF-9 is readily processed into the bioactive mature form, the processing of mouse BMP-15 pro-protein is impaired [13,42–44]. Furthermore, mouse oocytes could not activate the BMP signaling cascade in granulosa cells, and the mouse oocyte-stimulation of granulosa cell DNA synthesis is exclusively mediated through SMAD2/3 [45]. Because our ELISA assay revealed both GDF-9 and BMP-15 in POCM and the expression of both GDF-9 and BMP-15 has been observed in porcine oocytes [35,46], the current results suggest that in vivo, mouse oocytes prevent CC apoptosis mainly by secreting GDF-9 and that pig oocyte-secreted GDF-9 and BMP-15 can inhibit apoptosis of mouse CCs.

The current results suggest that OSFs including GDF-9 suppress apoptosis of CCs by upregulating miR-21 expression. Thus, although the level of miR-21 was significantly lower in OOXs than in COCs after culture in s-MEM alone, miR-21 levels increased significantly when OOXs were cultured in the presence of recombinant mouse GDF-9 or in POCM that contained GDF-9. Furthermore, while upregulating miR-21 expression reduced, downregulation of

miR-21 expression increased apoptosis of cultured CC monolayers significantly. There are many reports on the antiapoptotic effect of miR-21. For example, miR-21 levels were markedly elevated in tumor tissues [20–22]. Whereas miR-21 overexpression promoted proliferation and invasion and inhibited apoptosis, anti-miR-21 yielded apoptotic effects in colorectal cancer cells [23]. The expression of miR-21 has been reported in human CCs [16,47] and in mouse granulosa cells [24]. Furthermore, miR-21 blocked apoptosis in mouse periovulatory granulosa cells [24].

The present data indicate that both recombinant mouse GDF-9 and the POCM that contained GDF-9 inhibited apoptosis and elevated miR-21 levels in mouse CCs with activation of the TGF-β superfamily signaling. Thus, either inhibiting ALK5 with SB431542 or inhibiting SMAD3 with SIS3 completely abolished the beneficial effects of GDF-9 and POCM on CC apoptosis and miR-21 levels in the cultured mouse OOXs. Both GDF-9 and BMP-15 have been shown to signal through TGF-β superfamily receptors to activate the SMAD intracellular cascade in granulosa cells [15]. It has been reported that OSFs promoted mouse cumulus expansion through activation of the SMAD 2/3 signaling cascades [34]. Furthermore, in human vascular smooth muscle cells, the TGF-β signaling promotes a rapid increase in the expression of mature miR-21 through promoting the processing of pri-miR-21 into pre-miR-21 by the DROSHA complex [25]. However, our real-time PCR analysis did not reveal any increase in Drosha mRNA but instead demonstrated a close correlation between the level of miR-21 and that of Dicer1 mRNA in the OSF-treated CCs. It has been reported that p-SMAD2/3 interacts with DICER1 to promote pre-miR-21 processing to mature miR-21 in cardiac fibroblasts [48]. There are also reports that while the level of Drosha mRNA was upregulated, that of Dicer1 mRNA was downregulated in basal cell carcinomas cells [49] and in cells of oxygen-induced retinopathy [50]. Furthermore, DROSHA was induced by nutrient and energy deprivation and conferred resistance to glucose deprivation-induced apoptosis [51]. Taken together, it is suggested that the OSFs enhanced miR-21 processing in CCs through DICER but not through DROSHA, and that the expression of DROSHA may be promoted at the early stages of cell apoptosis.

In this study, when mouse OOXs were cultured with GDF-9, or when CC monolayers transfected with miR-21 mimic were cultured in s-MEM medium, the presence of PI3K inhibitor, LY294002, significantly increased CC apoptosis, suggesting that the OSF-upregulated miR-21 expression inhibits CC apoptosis by activating the PI3K/Akt signaling. In porcine CCs, GDF-9 maintained a low level of BIMEL expression and prevented apoptosis through activation of the PI3K/FOXO3a pathway [27]. Studies in other somatic cells also indicate that miR-21 inhibited apoptosis by upregulating the PI3K/Akt signaling pathway. For example, in human hepatic stellate LX-2 cells, overexpression of miR-21 decreased protein expression of phosphatase and tensin homolog (PTEN), resulting in activation of the Akt [29]. In nonsmall cell lung cancer A549 cells, miR-21 silencing sensitizes them to ionizing radiation-induced apoptosis through inhibition of the PI3K/Akt signaling [30]. Furthermore, miR-21 accelerated hepatocyte proliferation in vitro through the PI3K/Akt pathway by downregulating PTEN [31].

In summary, the evidence presented in the present paper demonstrates that miR-21 plays a pivotal role in the OSF inhibition of CC apoptosis. Thus, OSFs upregulated miR-21 expression through activation of TGF-β superfamily signaling, and miR-21 suppressed CC apoptosis by activating the PI3K/AKT signaling. Based on the data obtained, possible pathways for miR-21 upregulation and its inhibition on CC apoptosis were proposed (Figure 7). Thus, OSFs binding BMPRII/ALK5 leads to activation of ALK5, which in turn activates SMAD3. Activated SMAD3 promotes the processing of pre-miR-21 into mature miR-21 by interacting with DICER, leading to increased expression of miR-21. Increased miR-21 suppresses apoptosis with inactivation of caspase-3 and an increase in the Bcl2/Bax ratio by upregulating PI3K/Akt signaling through downregulating PTEN. The data are important for our understanding of the intracellular mechanisms by which OSFs inhibit CC apoptosis and can add to the growing list of miRNA functions in reproduction.

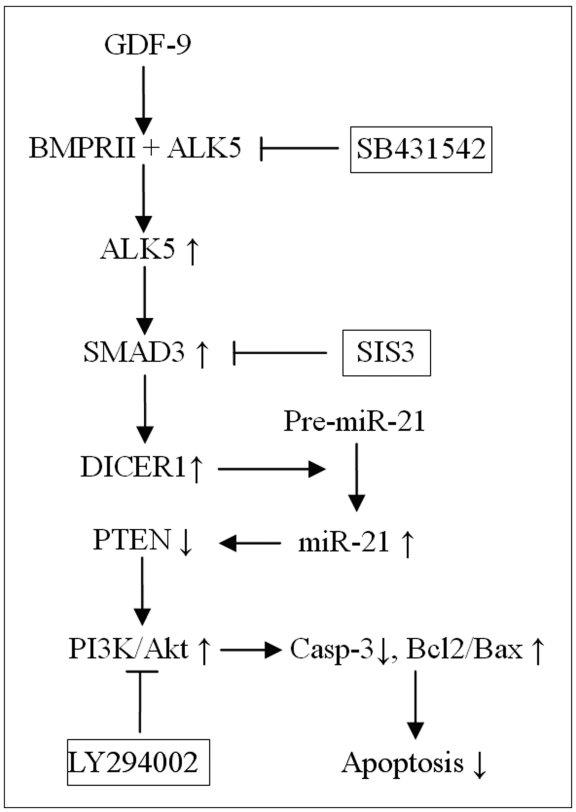

Figure 7. Proposed pathways for miR-21 upregulation and its inhibition on CC apoptosis. GDF-9 binding BMPRII/ALK5 leads to activation of ALK5, which in turn activates SMAD3. Activated SMAD3 promotes the processing of precursor miR-21 (pre-miR-21) into mature miR-21 by interacting with DICER, leading to increased expression of miR-21. Increased miR-21 suppresses apoptosis with inactivation of caspase-3 and an increase in the Bcl2/Bax ratio by upregulating PI3K/Akt signaling via downregulating phosphatase and tensin homolog (PTEN). Of the three inhibitors used in this study, SB431542 is an inhibitor of ALK5, which prevents the association between ALK5 and BMPRII, SIS3 prevents the phosphorylation (activation) of SMAD3, and LY294002 inhibits phosphatidylinositol 3-kinase (PI3K); all facilitate CC apoptosis.

Supplementary data

Supplementary data are available at *BIOLRE* online.

Supplementary Figure S1. Culture and transfection of CCs. Panel A shows a timetable for CC culture and transfection with miR-21 inhibitor or mimic. For transfection, CCs were first cultured in DMEM for 48 h, and then cultured in the transfection mix for 48 h before the test culture in s-MEM with or without GDF-9 for 24 or 48 h. Control CCs were cultured in DMEM continuously for 96 h before the test culture. '*' indicates the time when monolayers were formed with about 90% confluence. Panel B shows levels of

HAS2 mRNA in CCs after test culture in TCM-199 for 24 h with or without FSH in the presence of GDF-9 following culture in DMEM for 48 or 96 h. COC and COCF: COCs were test-cultured for 18 h without or with FSH, respectively; CC48, CC48G, and CC48GF: CCs were test-cultured with neither FSH nor GDF-9, with GDF-9 alone or with both FSH and GDF-9, respectively, after culture in DMEM for 48 h; CC96G and CC96GF: CCs were test-cultured with GDF-9 alone or with both FSH and GDF-9, respectively, after culture in DMEM for 96 h. The relative quantity value of HAS2 mRNA in COCs test-cultured without FSH was set as 1, and other values were expressed relative to this quantity. a, b: values with a different letter above their bars differ significantly ($P < 0.05$).

Supplemental Table S1. Details of antibodies used in this study.

References

1. Byskov AG. Follicular atresia. In: Jones RE (ed.), *The Vertebrate Ovary*. New York: Plenum Press; 1978:533–562.
2. Hirshfield AN, Midgley AR, Jr. Morphometric analysis of follicular development in the rat. *Biol Reprod* 1978; **19**:597–605.
3. Kruip TA, Dieleman SJ. Macroscopic classification of bovine follicles and its validation by micromorphological and steroid biochemical procedures. *Reprod Nutr Dev* 1982; **22**:465–473.
4. Blondin P, Dufour M, Sirard MA. Analysis of atresia in bovine follicles using different methods: flow cytometry, enzyme-linked immunosorbent assay, and classic histology. *Biol Reprod* 1996; **54**:631–637.
5. Irving-Rodgers HF, van Wezel IL, Mussard ML, Kinder JE, Rodgers RJ. Atresia revisited: two basic patterns of atresia of bovine antral follicles. *Reproduction* 2001; **122**:761–775.
6. Driancourt MA, Fair T, Reynaud K. Oocyte apoptosis: when, how, why?. *Contracept Fertil Sex* 1998; **26**:522–527.
7. Leibfried L, First NL. Characterization of bovine follicular oocytes and their ability to mature in vitro. *J Anim Sci* 1979; **48**:76–86.
8. Driancourt M. Follicular dynamics in sheep and cattle. *Theriogenology* 1991; **35**:55–79.
9. Hussein TS, Froiland DA, Amato F, Thompson JG, Gilchrist RB. Oocytes prevent cumulus cell apoptosis by maintaining a morphogenic paracrine gradient of bone morphogenetic proteins. *J Cell Sci* 2005; **118**(Pt 22):5257–5268.
10. Su YQ, Wu X, O'Brien MJ, Pendola FL, Denegre JN, Matzuk MM, Eppig JJ. Synergistic roles of BMP15 and GDF9 in the development and function of the oocyte-cumulus cell complex in mice: genetic evidence for an oocyte-granulosa cell regulatory loop. *Dev Biol* 2004; **276**: 64–73.
11. Mester B, Ritter LJ, Pitman JL, Bibby AH, Gilchrist RB, McNatty KP, Juengel JL, McIntosh CJ. Oocyte expression, secretion and somatic cell interaction of mouse bone morphogenetic protein 15 during the periovulatory period. *Reprod Fertil Dev* 2015; **27**:801–811.
12. McGrath SA, Esquela AF, Lee SJ. Oocyte-specific expression of growth/differentiation factor-9. *Mol Endocrinol* 1995; **9**:131–136.
13. Elvin JA, Clark AT, Wang P, Wolfman NM, Matzuk MM. Paracrine actions of growth differentiation factor-9 in the mammalian ovary. *Mol Endocrinol* 1999; **13**:1035–1048.
14. Elvin JA, Yan C, Matzuk MM. Oocyte-expressed TGF-beta superfamily members in female fertility. *Mol Cell Endocrinol* 2000; **159**: 1–5.
15. Gilchrist RB, Lane M, Thompson JG. Oocyte-secreted factors: regulators of cumulus cell function and oocyte quality. *Hum Reprod Update* 2008; **14**:159–177.
16. Assou S, Al-edani T, Haouzi D, Philippe N, Lecellier CH, Piquemal D, Commes T, Aït-Ahmed O, Dechaud H, Hamamah S. MicroRNAs: new candidates for the regulation of the human cumulus-oocyte complex. *Hum Reprod* 2013; **28**:3038–3049.
17. Abd El Naby WS, Hagos TH, Hossain MM, Salilew-Wondim D, Gad AY, Rings F, Cinar MU, Tholen E, Looft C, Schellander K, Hoelker M, Tesfaye D. Expression analysis of regulatory microRNAs in bovine cumulus oocyte complex and preimplantation embryos. *Zygote* 2013; **21**:31–51.
18. Yao G, Liang M, Liang N, Yin M, Lü M, Lian J, Wang Y, Sun F. MicroRNA-224 is involved in the regulation of mouse cumulus expansion by targeting Ptx3. *Mol Cell Endocrinol* 2014; **382**:244–253.
19. Pan B, Toms D, Shen W, Li J. MicroRNA-378 regulates oocyte maturation via the suppression of aromatase in porcine cumulus cells. *Am J Physiol Endocrinol Metab* 2015; **308**:E525–534.
20. Chan JA, Krichevsky AM, Kosik KS. MicroRNA-21 is an antiapoptotic factor in human glioblastoma cells. *Cancer Res* 2005; **65**:6029–6033.
21. Yang CH, Yue J, Pfeffer SR, Fan M, Paulus E, Hosni-Ahmed A, Sims M, Qayyum S, Davidoff AM, Handorf CR, Pfeffer LM. MicroRNA-21 promotes glioblastoma tumorigenesis by down-regulating insulin-like growth factor-binding protein-3 (IGFBP3). *J Biol Chem* 2014; **289**:25079–25087.
22. Si ML, Zhu S, Wu H, Lu Z, Wu F, Mo YY. miR-21-mediated tumor growth. *Oncogene* 2007; **26**:2799–2803.
23. Liu M, Tang Q, Qiu M, Lang N, Li M, Zheng Y, Bi F. miR-21 targets the tumor suppressor RhoB and regulates proliferation, invasion and apoptosis in colorectal cancer cells. *FEBS Lett* 2011; **585**:2998–3005.
24. Carletti MZ, Fiedler SD, Christenson LK. MicroRNA 21 blocks apoptosis in mouse periovulatory granulosa cells. *Biol Reprod* 2010; **83**:286–295.
25. Davis BN, Hilyard AC, Lagna G, Hata A. SMAD proteins control DROSHA-mediated microRNA maturation. *Nature* 2008; **454**(7200):56–61.
26. Zhong X, Chung AC, Chen HY, Meng XM, Lan HY. Smad3-mediated upregulation of miR-21 promotes renal fibrosis. *J Am Soc Nephrol* 2011; **22**:1668–1681.
27. Wang XL, Wang K, Zhao S, Wu Y, Gao H, Zeng SM. Oocyte-secreted growth differentiation factor 9 inhibits BCL-2-interacting mediator of cell death-extra long expression in porcine cumulus cell. *Biol Reprod* 2013; **89**:56.
28. Li Z, Zhang P, Zhang Z, Pan B, Chao H, Li L, Pan Q, Shen W. A co-culture system with preantral follicular granulosa cells in vitro induces meiotic maturation of immature oocytes. *Histochem Cell Biol* 2011; **135**:513–522.
29. Wei J, Feng L, Li Z, Xu G, Fan X. MicroRNA-21 activates hepatic stellate cells via PTEN/Akt signaling. *Biomed Pharmacother* 2013; **67**:387–392.
30. Ma Y, Xia H, Liu Y, Li M. Silencing miR-21 sensitizes non-small cell lung cancer A549 cells to ionizing radiation through inhibition of PI3K/Akt. *Biomed Res Int* 2014; **2014**:617868.
31. Yan-nan B, Zhao-yan Y, Li-xi L, jiang Y, Qing-jie X, Yong Z. MicroRNA-21 accelerates hepatocyte proliferation in vitro via PI3K/Akt signaling by targeting PTEN. *Biochem Biophys Res Commun* 2014; **443**:802–807.
32. Richards JS. Ovulation: new factors that prepare the oocyte for fertilization. *Mol Cell Endocrinol* 2005; **234**:75–79.
33. Liu J, Tu F, Yao W, Li X, Xie Z, Liu H, Li Q, Pan Z. Conserved miR-26b enhances ovarian granulosa cell apoptosis through HAS2-HA-CD44-Caspase-3 pathway by targeting HAS2. *Sci Rep* 2016; **6**:21197.
34. Dragovic RA, Ritter LJ, Schulz SJ, Amato F, Thompson JG, Armstrong DT, Gilchrist RB. Oocyte-secreted factor activation of SMAD 2/3 signaling enables initiation of mouse cumulus cell expansion. *Biol Reprod* 2007; **76**:848–857.
35. Lin ZL, Li YH, Xu YN, Wang QL, Namgoong S, Cui XS, Kim NH. Effects of growth differentiation factor 9 and bone morphogenetic protein 15 on the in vitro maturation of porcine oocytes. *Reprod Domest Anim* 2014; **49**:219–227.
36. Gilchrist RB, Ritter LJ, Myllymaa S, Kaivo-Oja N, Dragovic RA, Hickey TE, Ritvos O, Mottershead DG. Molecular basis of oocyte-paracrine signalling that promotes granulosa cell proliferation. *J Cell Sci* 2006; **119**(Pt 18):3811–3821.
37. McNatty KP, Juengel JL, Reader KL, Lun S, Myllymaa S, Lawrence SB, Western A, Meerasahib MF, Mottershead DG, Groome NP, Ritvos O, Laitinen MP. Bone morphogenetic protein 15 and growth differentiation factor 9 co-operate to regulate granulosa cell function in ruminants. *Reproduction* 2005; **129**:481–487.
38. Orisaka M, Orisaka S, Jiang JY, Craig J, Wang Y, Kotsuji F, Tsang BK. Growth differentiation factor 9 is antiapoptotic during follicular development from preantral to early antral stage. *Mol Endocrinol* 2006; **20**:2456–2468.

39. Zhai B, Liu H, Li X, Dai L, Gao Y, Li C, Zhang L, Ding Y, Yu X, Zhang J. BMP15 prevents cumulus cell apoptosis through CCL2 and FBN1 in porcine ovaries. *Cell Physiol Biochem* 2013; **32**:264–278.
40. Dube JL, Wang P, Elvin J, Lyons KM, Celeste AJ, Matzuk MM. The bone morphogenetic protein 15 gene is X-linked and expressed in oocytes. *Mol Endocrinol* 1998; **12**:1809–1817.
41. Yoshino O, McMahon HE, Sharma S, Shimasaki S. A unique preovulatory expression pattern plays a key role in the physiological functions of BMP-15 in the mouse. *Proc Natl Acad Sci USA* 2006; **103**:10678–10683.
42. Liao WX, Moore RK, Shimasaki S. Functional and molecular characterization of naturally occurring mutations in the oocyte-secreted factors bone morphogenetic protein-15 and growth and differentiation factor-9. *J Biol Chem* 2004; **279**:17391–17396.
43. Hashimoto O, Moore RK, Shimasaki S. Posttranslational processing of mouse and human BMP-15: potential implication in the determination of ovulation quota. *Proc Natl Acad Sci USA* 2005; **102**:5426–5431.
44. McNatty KP, Juengel JL, Reader KL, Lun S, Myllymaa S, Lawrence SB, Western A, Meerasahib MF, Mottershead DG, Groome NP, Ritvos O, Laitinen MP. Bone morphogenetic protein 15 and growth differentiation factor 9 co-operate to regulate granulosa cell function. *Reproduction* 2005; **129**:473–480.
45. Gilchrist RB, Ritter LJ, Myllymaa S, Kaivo-Oja N, Dragovic RA, Hickey TE, Ritvos O, Mottershead DG. Molecular basis of oocyte-paracrine signalling that promotes granulosa cell proliferation. *J Cell Sci* 2006; **119**(Pt 18):3811–3821.
46. Saadeldin IM, Elsayed A, Kim SJ, Moon JH, Lee BC. A spatial model showing differences between juxtacrine and paracrine mutual oocyte-granulosa cells interactions. *Indian J Exp Biol* 2015; **53**:75–81.
47. Karakaya C, Guzeloglu-Kayisli O, Uyar A, Kallen AN, Babayev E, Bozkurt N, Unsal E, Karabacak O, Seli E. Poor ovarian response in women undergoing in vitro fertilization is associated with altered microRNA expression in cumulus cells. *Fertil Steril* 2015; **103**:1469–1476.
48. García R, Nistal JF, Merino D, Price NL, Fernández-Hernando C, Beaumont J, González A, Hurlé MA, Villar AV. p-SMAD2/3 and DICER promote pre-miR-21 processing during pressure overload-associated myocardial remodeling. *Biochim Biophys Acta* 2015; **1852**:1520–1530.
49. Sand M, Gambichler T, Skrygan M, Sand D, Scola N, Altmeyer P, Bechara FG. Expression levels of the microRNA processing enzymes Drosha and dicer in epithelial skin cancer. *Cancer Invest* 2010; **28**:649–653.
50. Liu CH, Wang Z, Sun Y, SanGiovanni JP, Chen J. Retinal expression of small non-coding RNAs in a murine model of proliferative retinopathy. *Sci Rep* 2016; **6**:33947.
51. Ye P, Liu Y, Chen C, Tang F, Wu Q, Wang X, Liu CG, Liu X, Liu R, Liu Y, Zheng P. An mTORC1-Mdm2-Drosha axis for miRNA biogenesis in response to glucose- and amino acid-deprivation. *Mol Cell* 2015; **57**:708–720.